Underwater Image Enhancement using Fusion of CLAHE and Total Generalized Variation

T. Surya Kavitha, *Member, IAENG,* A. Vamsidhar*, *Member, IAENG,* G. Sunil Kumar, *Member, IAENG,* R. Viswanadham, V. Anand Kumar and T. Madhuri

***Abstract*— In order to learn more about the volcanic eruptions and sea creatures on the seabed, the underwater images are a great resource. When light travels from air to water, which is denser comparatively, it scatters and bends, causing several kinds of issues. The primary difficulties of an underwater image are its inadequate contrast, colour distortion, and poor visual quality. Even the sea water marine life also plays a vital role on poor quality of underwater images. In this study, a new approach is proposed for developing underwater images by combining Contrast-Limited Adaptive Histogram Equalization (CLAHE) and Total Generalized Variation (TGV) methods. The suggested fusion approach takes an underwater image as input and processes it using CLAHE and TGV. The initial stage is white balancing the color-distorted input image to eliminate colour casts while retaining a realistic underwater image. Underwater pictures may be greatly improved by applying CLAHE to the gamma-corrected picture, and TGV can be used to eliminate extraneous detail from an image while keeping vital elements like edges intact. Here, the performance metrics like UCIQE (Underwater Colour Image Quality Evaluation Metric), UIQM (Underwater Image Quality Measure), PCQI (Patch-based Contrast Quality Index) are employed to estimate the quality of the enhanced images, and PSNR (Peak Signal-to-Noise Ratio), SSIM (Structural Similarity Index Measure) are estimated to find the amount of noise components present in the enhanced underwater image. We found that the results are appreciable with the cascaded approach compared to the exiting methods.**

***Index Terms*—Underwater image enhancement, CLAHE, Total Generalized Variation, UCIQE, UIQM, PCQI**

I. INTRODUCTION

In the past 20 years, interest in ocean investigation and marine robotics has grown tremendously. As a result, aquatic robotics has significantly advanced, allowing them to carry out more difficult tasks underwater on their own [1]. Thus, research using AUVs (Autonomous underwater vehicles) deep into the sea made underwater image processing crucial in the process. Algorithms for underwater image processing are now employed in applications such as underwater mine detection, underwater imaging, underwater archaeology, mapping ocean basements, and submerged robotics [2]. The most critical issue is improving underwater imagery quality to optimize image processing analysis. Problems associated with underwater imaging arise from the effects of light absorption and scattering through marine environment. Nevertheless, these technologies have still not reached the proper mode of successful [3]. For example, automatic underwater vehicle movement creates shadows in the scene, but using an optical camera to capture underwater images has a limited field of view. It contains its own advantages and disadvantages.

To overwhelm these limitations, this manuscript proposes a fusion technique of CLAHE [4, 5] and Total Generalized Variation (TGV) [6, 7] for the enhancement of underwater images. The key contributions of this manuscript are abridged below,

- A fusion technique of CLAHE and TGV method is proposed for the enhancement of underwater images.
- Firstly, use CLAHE approach for equalizing the colour contrast on images.
- Second, apply the Total Generalized Variation (TGV) to maximize the real colour and deal the issue of lighting.

Though these two methods were applied independently for image enhancement by many researchers, but cascading them is a novel and effective approach, as proven in this work. An underwater image is passed through the process of white balancing, gamma correction and sharpening before the fusion technique is applied. CLAHE is applied to the gamma corrected picture for enhancing the brightness of underwater images, while TGV is a noise removal filter. TGV is subject to enhanced image being a close match to the original underwater image by removing the unwanted details while retaining the original ones such as edges. The

Manuscript received January 23, 2023; revised August 14, 2023.

T. Surya Kavitha is an Associate Professor of ECE Department, Raghu Engineering College, Visakhapatnam, INDIA 531162. (e-mail: kavitats24@gmail.com).

*A. Vamsidhar is an Associate Professor of ECE Department, Raghu Engineering College, Visakhapatnam, INDIA 531162. (Phone: +91-9849332767; e-mail: vamsianagani@gmail.com).

G. Sunil Kumar is an Assistant Professor of ECE Department, Raghu Engineering College, Visakhapatnam, INDIA 531162. (e-mail: sunil.suni211@gmail.com).

R. Viswanadham is an Associate Professor of ECE Department, BVRIT Hyderabad College of Engineering for Women, Hyderabad, INDIA 500090. (e-mail: viswamravuri@gmail.com).

V. Anand Kumar is an undergraduate student of ECE Department, Raghu Engineering College, Visakhapatnam, INDIA 531162. (e-mail: anandkumarvellampalli@gmail.com).

T. Madhuri is an undergraduate student of ECE Department, Raghu Engineering College, Visakhapatnam, INDIA 531162. (e-mail: madhuritirumareddy99@gmail.com).

parameters UCIQE (Underwater Colour Image Quality Evaluation), UIQM (Underwater Image Quality Measure), PCQI (Patch-based Contrast Quality Index) are employed to estimate the quality of the enhanced images, where PSNR (Peak Signal-to-Noise Ratio), SSIM (Structural Similarity Index Measure). Average Gradient (AG), RMSE (Root Mean Squared-Error), Sobel Count and Entropy are measured to find the amount of noise components present in the enhanced underwater image. The proposed method is comparing to the existing models, like Retinex [8], DCP (Dark Channel Prior) [9, 10] and CLAHE [5], and found that the results obtained are far better than its counterparts.

Remaining manuscript is arranged as follows: Section II discusses the state-of-the-art in terms of underwater image enhancement research, Section III provides a system model for the scattering of light under seawater, Section IV demonstrates the approach of the proposed cascaded enhancement method on underwater images, Section V presents experimental results with both qualitative and quantitative analysis, and Section VI draws a conclusion.

II. Literature Review

There are many research applications done using different methods for the underwater image enhancement. Though many methods provide a good picture output, still they lack in atleast one of the metric values in the quantitative analysis, making it difficult for any further refinement in image processing. Let discuss some of the previous methods in terms of underwater image enhancement research.

- Wei Song *et al.* [11] suggested a promising method for developing underwater images, which included underwater image restoration and a simple colour correction depending on white balancing with optimal gain factor, using novel statistical models of Background Lights and optimal Transmission Map assessment models.
- Using a fusion technique based upon weighted maps generated by integrating the attributes of global contrast, local contrast, saliency, and exposedness, Yue Zhang *et al.* [12] suggested an enhanced method for removing the local reddish effect with sinking image noise.
- A useful approach for assessing the efficiency of underwater picture enhancement methods was first defined by Marino Mangeruga *et al.* [13]. It helped to figure out which method would work best for a certain task under different underwater conditions.
- By combining the benefits of multiscale fusion and contrast enhancement methodologies, Sangeetha Mohan *et al.* [14] suggested a way to recover underwater photographs with high precision.
- By first applying the enhancement algorithm to the vague underwater image, adjusting the white-balance and contrast, calculating the weight maps for both strategies, and then fusing the images using the fusion strategy, Aashi Singh *et al.* [15] presented an effective algorithm for underwater image enhancement.
- The simple and effective approach for dehazing underwater images developed by Belsare *et al.* [16] involves modifying the traces of the transmission map of a picture using a Gaussian low-pass filter. In addition, enhancements to underwater images in real time are achieved via the use of the Dark Channel and atmospheric light computation.
- The approach developed by Aruna Bhat *et al.* [17], which uses histogram equalisation methods for image de-hazing and white balanced techniques for colour correction and was rapid enough for real-time schemes, like AUVs and ROVs (Remotely Operated Vehicles).
- Sun Bo *et al.* [18] exhibited a unique method for enhancing underwater images by calculating the background lighting of the water object in the uploaded underwater picture and matching the predicted value with the predefined essential brightness value.
- A new method for improving underwater images was presented by Sourav De *et al.* [19], which involves splitting pixels in half and then applying a variant of the Artificial Bee Colony (ABC) algorithm to boost their construction levels.
- Chongyi Li *et al.* [20] established Underwater Image Enhancement Benchmark data collection comprising large-scale authentic underwater and reference imageries. To train CNNs for underwater picture enhancement using this benchmark dataset.
- With regards to dehazing underwater images, Ramkumar *et al.* [21] suggested a revolutionary CNN-based Deep Learning technique.
- A box-based image improvement approach and the Retinex image enhancement method based on optical analysis were proposed by Lixue Xu *et al.* [22] to address the issues of low-quality underwater images.
- A unique stationary wavelet based fusion strategy was presented by Sonal Yadav *et al.* [23] to enhance the quality and clarity of individual underwater photos. The primary goal of the suggested model was to address the issues of colour cast, noise, and distortion in underwater images.
- Zhao *et al*. [24] suggested a novel variation approach that uses Retinex with a TGV prior on the lighting to enhance the quality of blemished underwater images. Total Variation (TV) prior was combined with 1st and 2nd order TV to approximate the smoothness of piecewise and piecewise linear respectively, in the model of light intensity variation.

III. System Model

Compared to air, water is several hundred times denser. Hence, the transportation properties of light in an underwater environment present a difficult task for picture enhancement. Significant energy is lost when light travels through water, resulting in poor colour and contrast in underwater images, which distorts the information contained in the image [25]. Artificial illumination was suggested as a solution to this issue, however this led to another issue that creates a high intensity in the center of the image, and as we travel away from the center, the intensity decreases, creating a non-uniform illumination [26]. Along with uneven illumination, the peculiar absorption and scattering

properties of light along with Backscattering and Marine snow also contribute to the deterioration of underwater images.

Absorption: At certain depths under water, particular wavelengths of light are absorbed. Red absorbs far more than green and blue at much shallower depths. In the majority of underwater photographs, this causes a blue or green colour cast [27].

Scattering: Particles suspended underwater are far bigger than those found in the air due to scattering. Dim pictures are the result of incident light reflected from objects being scattered by particles. This process results in the loss of contrast and edges [28].

Backscattering: When artificial light illuminates suspended particles, the ensuing noise in underwater photos makes it difficult to perform tasks like segmentation.

Marine Snow: Microscopic fragments of inorganic or biological material that can be seen in underwater pictures of seas, thus adding more noise to the underwater images [29].

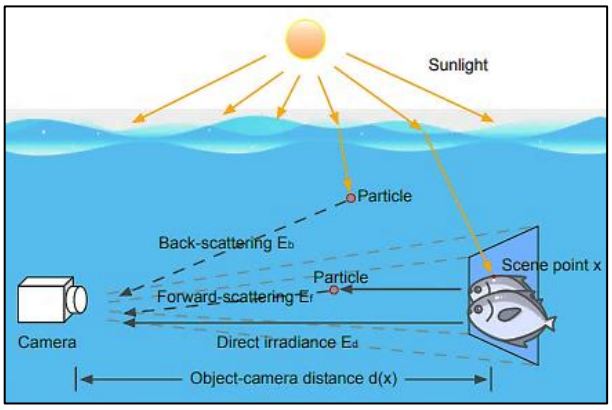

Fig. 1. Underwater image showing the scattering of light under water with an Object-camera distance as $d(x)$

Fig.1 illustrates the underwater image model suggested by McGlamery [30], which states that the majority of illumination acquired by the underwater imaging system is believed to be composed mainly of three important components: (i) Light that is reflected directly from an object is called the direct component E_d; (ii) Light that is scattered far from propagation trajectory but still reaches the imaging equipment is called forward-scattering component E_f; and (iii) Light is scattered by particles in the air is called the back-scattering component E_b. The aforementioned three components can be interpreted as a linear superposition to represent the complete optical radiation E_T, given as:

$$E_T(x,y) = E_d(x,y) + E_f(x,y) + E_b(x,y) \quad (1)$$

Where (x,y) denotes pixel's coordinates in the underwater picture. The component E_f may be disregarded since the scene under the water and camera are quite nearer, resulting in the following representation of scene $I(x,y)$ that the camera recorded:

$$I^c(x,y) = E_d(x,y) + E_b(x,y) \quad (2)$$

Here $c \in \{r,g,b\}$ means red, green and blue colour components respectively. If we write $I(x,y)$ as the scene intensity and define $J(x,y)$ as scene radiance, $t(x,y)$ as transmission that decreases in an exponential fashion with depth, B as background light [31]:

$$I^c(x,y) = J^c(x,y)t^c(x,y) + B^c(1 - t^c(x,y)) \quad (3)$$

In most cases, the optimized model for underwater imaging (3) is considered to be equivalent to the atmospheric optical imaging model. Thus, external picture restoration methods are being gradually implemented to introduce underwater scenes. Light is absorbed differently by different wavelengths in water. Red light absorbs faster in water due to its longer wavelength than green and blue light, giving underwater scenes a bluish-green hue. Extreme attenuation of a single colour channel can have a large effect on the success of several existing outdoor restoration methods. There have been a lot of different suggestions about how to make underwater images look better.

IV. Proposed Method

Here, we offer a method for improving real-world underwater photographs that makes use of a fusion technique of CLAHE [5] and TGV [7] to restore brightness, colour, and contrast all at once. The component of the work that contributes is the contrast enhancement. Histogram methods are used to produce the contrast enhancement. The brightness is improved using CLAHE, and the image is sharpened before histogram linearization is employed. This improvement increases the image's contrast using the input image as a starting point. On the illumination, TGV is utilized for approximating the piecewise smoothness as well as piecewise linear smoothness of illumination [24]. The suggested strategy allows for the visualization of finer details and the framework is depicted in Fig.2.

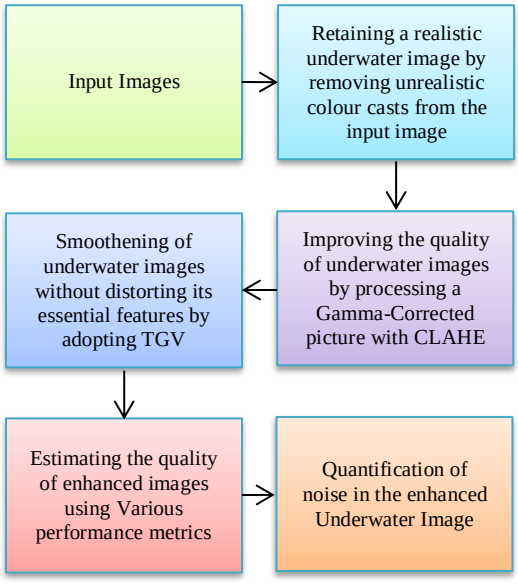

Fig. 2. Framework showing the process of underwater image enhancement depends on proposed method

In underwater, as per the electromagnetic spectrum, red is more dominating than green and blue colors, and this dominated image sharpness, so image colors change with distance in terms of depth. Sharpening and gamma correction are applied after the white-balanced image has been processed. The images are then sent to a module for improvement, and finally the images are enhanced using CLAHE [5] and TGV [7]. The following is a discussion of the different steps in the proposed method:

A. White Balance

White balancing refers to the technique of eliminating the colour cast from pictures. The dominance of a certain colour in the scene at the time the image was taken causes colour casts or colour distortion in images. Simplest colour balancing, Grey world, Robust Auto White balance, and Sensor Correlation are some colour balancing algorithms. The impact of colour recognition and identification underwater is influenced by depth. The colour of underwater photos, which leans greenish-blue, is a major problem that has to be fixed. In our work, the Grey World algorithm is used because it effectively removes the blue tone found in underwater images, assuming that an image's light reflectance is achromatic or colorless. The Grey World algorithm has a flaw that it has strong red artefacts. Due to the red channel's comparative low mean value, it overcompensates in regions where red is predominated, which causes these distortions. Every channel is divided by the mean value using the Grey world algorithm. Following the recommendations from earlier underwater research, the primary goal is to make up for the loss of red channel in order to evade this problem. The Grey World technique determine the white balanced picture then applied to create red channel compensation in the second stage. At every pixel location x, compensated red channel I_{rc} is represented as follows [32]:

$$I_{rc}(x) = I_r(x) + \alpha.\left(\bar{I}_g - \bar{I}_r\right).\left(1 - I_r(x)\right).I_g(x) \qquad (4)$$

After being normalized by the upper limit of their dynamic range, the red and green colour channels of image I are represented by I_r and I_g in the range [0,1] for each channel, whereas $\bar{I}_r$ and $\bar{I}_g$ signify the mean value of I_r and I_g respectively. Absorption of the blue channel by organic matter can significantly weaken its intensity in murky waters and in areas with a high concentration of plankton. Here, this is determined that compensating the red channel is not adequate, then that the blue channel also needs compensation in order to lessen its attenuation [33]. Due to the blue channel's absorption by organic matter, it may be significantly diminished in areas with high plankton density or murky waters. Here, it is discovered that the red channel compensation is inadequate, necessitating the compensation of the blue channel to lessen its attenuation. The Grey World algorithm-based white balancing process then occurs.

B. Gamma Correction

After a process of white balancing, an output is generated and its hue is modified. Given that a properly white-balanced image isn't enough to bring back the absorbed colour in underwater photographs, we supplement it with a gamma correction. Because white-balanced images typically look too bright, gamma correction is used to modify the overall contrast. In any case, gamma correction tends to hide details in the image that are too dark or too bright. Sharpening helps bring back some of the lost detail.

C. Sharpening

When unsharp masking is employed, the white balanced image becomes sharper. Unsharp masking creates an image with sharper edges, corners, limits, and other finer details by subtraction the lesser pass version of image from the original. The following formula produces a filtered image with a high pass frequency as a result:

$$S = I + \beta(I - (G * I)) \qquad (5)$$

Where I stands for the image to be sharpened, $G * I$ represents the image I after a Gaussian filter, β is a parameter that, sharpens the image when to its minimum value, and when set to its maximum value, causes oversaturation. Hence, the unsharp masking is carried out as shown below:

$$S = \frac{(I + N\{I - G * I\})}{2} \qquad (6)$$

Where N denotes normalization operator. The unsharp masking process makes use of a 3×3 Gaussian filter.

D. Total Generalized Variation (TGV)

TGV, originally invented by Bredies *et al.* [7], is an expansion of the concept of total variation (TV). Subsequently, numerous researchers have taken TGV and applied it to the realm of image processing. Rather than relying on a predefined combination, TGV is made up of polynomials of any order that may reconstruct piecewise polynomial functioning and balanced first and higher-order variants automatically. TGV can be thought of as a union of smoothness of any order (from first order smoothness on up). First-order variations are used to keep details crisp, while higher-order variations are used to effectively mimic smooth transition areas [34]. Therefore, stair-like artefacts are avoided. The TV was first introduced by Rudin *et al.* [35], which kicked off a new trend in using variational methods in image processing. Edge recovery, one of the most crucial aspects of image analysis, has seen extensive application in TV. For an image $u: \Omega \to R$, TV of u is defined as follows:

$$\mathrm{TV}(u) = \int_{\Omega} |\nabla u| \qquad (7)$$

TVs staircase artefacts in the smooth transition areas of images are well-known to be a downside, because TV favors solutions are piecewise constant. Total generalized variation (TGV) is a more general variational method developed to solve this issue [36]. In principle, TGV has the ability to quantify image properties up to a fixed level of discrimination. It was demonstrated that the 1st order TGV is parallel to TV. TGV's higher-order feature, allows it to efficiently remove staircase artifacts. However, if the order of the TGV is too high, it becomes computationally expensive and tough to discretize. The 2nd order TGV is

considered here because of trade-off it provides betwixt computation complex and quantitative precision. For image u, the 2nd order TGV is formulated as

$$\mathrm{TGV}(u) = \min_{v} \left\{ \alpha_1 \int_{\Omega} |\nabla u - v| + \alpha_0 \int_{\Omega} |\xi(v)| \right\} \quad (8)$$

Where, $\xi(v) = \frac{1}{2}(\nabla v + \nabla v^T)$ denotes the distributional symmetrized derivative and $\alpha_0, \alpha_1 \epsilon \mathbb{R}^+$ are weights. Concatenating the columns of the 2-tensor v creates a vector for computational ease.

E. Contrast Limited Adaptive Histogram Equalization (CLAHE)

Underwater images can be difficult to capture because of the uneven lighting conditions. An image's brightness is increased so that it can surpass this barrier. CLAHE is crucial in improving the brightness of marine photography. After the white-balanced image has been gamma-corrected, TGV and CLAHE are used to increase the brightness. Histogram equalization is a method for balancing out intensity levels across a specified interval. In lieu of retrieving information from entire image to create equalization functioning, the adaptive histogram equalization (AHE) creates independent histograms for each region of the image and then adjusts the contrast between them. But in relatively homogeneous regions, noise amplification can occur, making AHE less effective. Consequently, employ a variant of AHE termed as CLAHE. If AHE causes an over amplification, CLAHE can be used to correct it by clipping the histogram at predetermined value before calculating cumulative distribution function (CDF). The method employed in implementing CLAHE is obtained from [25]. The pixel intensity F_k frequency on the image may be defined by taking into account that the intensity values might range from 0 to 255 as:

$$F_k = n_k; 0 \leq k \leq 255 \quad (9)$$

Where n_k denotes the number of pixels whose intensities add up to k. CDF of intensity value at F_k is given in (10),

$$\mathrm{cdf}_{I(x,y)} = \sum_{k}^{I(x,y)} F_k \quad (10)$$

Where x denotes number of rows (1 to M), y denotes number of columns (1 to N). Now that each pixel's Histogram equalized Intensity value has been determined as,

$$I'(x,y) = \left\{ \frac{\left(\mathrm{cdf}_{I(x,y)} - \mathrm{cdf}_{min}\right)}{M \times N - \mathrm{cdf}_{min})} \times 255 \right\} \quad (11)$$

V. Simulated Results

A. Quantitative Analysis

There are a number of criteria that can be used to rate the efficacy of underwater augmentation. To quantitatively assess the effectiveness of the proposed technique, this work employs full-reference analysis (UCIQE, UIQM, PCQI) and non-reference analysis (PSNR, SSIM, RMSE, AG, Sobel Count, Entropy). We evaluate the restored photos against the reference images that UIEB provides, calculating the PSNR and PCQI to provide a complete picture of how well they matchup. Let us having a quick reference through the metrics mentioned:

UCIQE: It is a tool used is to estimate the observed images of underwater. It deems a linear combination of chroma, saturation and contrast to measure the non-uniform color cast, blur, and lower contrast. UCIQE is represented as:

$$\mathrm{UCIQE} = c_1 * \sigma_c + c_2 * con_1 + c_3 * \mu_s \quad (12)$$

Let σ_c, con_1 and μ_s specifies standard deviation of chroma, the contrast of luminance and average of saturation respectively. For this paper, the values of c_1, c_2 and c_3 are chosen as c_1= 0.4680, c_2= 0.2745, and c_3= 0.2576.

UIQM: It comprises three classifier measurements: underwater image colorfulness measure (UICM), underwater image sharpness measure (UISM), underwater image contrast measure (UIConM) [33].

- *UICM*: The hue of many underwater photographs is drastically off. One by one, the wavelengths of colours are absorbed by the deeper the water becomes. Since red has the shortest wavelength, it is the first hue to fade away. As a result, pictures taken underwater tend to seem blue or greenish. Underwater photographs suffer from extreme colour desaturation because of the lack of available light. If you want to improve your underwater photos, go for one with accurate colours.
- *UISM*: Sharpness is the quality that ensures the integrity of fine distinctions and edges. When taking pictures underwater, forward scattering causes significant blurring [12]. The loss of detail in the image is a result of the blurring effect.
- *UIConM*: Underwater visual performance, including stereoscopic acuity, has been found to correlate with contrast. Backscattering is typically to blame for the loss of contrast in underwater photographs.

The linear superposition of absorbed and dispersed components has been demonstrated to be a valid model for describing underwater images. It is also widely recognized that the effects of absorption and scattering reduce colour, sharpness, and contrast. To make the entire measure of underwater image quality, this is sense to employ the linear superposition model. The overall UIQM is then given by [37]:

$$\mathrm{UIQM} = c_1 * \mathrm{UICM} + c_2 * \mathrm{UISM} + c_3 * \mathrm{UIConM} \quad (13)$$

Where metrics of colour vibrancy, image clarity, and contrast are linearly added. It is important to note that the UIQM in (12) relies on three factors, denoted c_1, c_2 and c_3. These settings are chosen on a case-by-case basis. For underwater picture colour correction, for instance, the UICM should be given more weights, whereas UIConM and UISM should be given more weights when trying to improve underwater image visibility. Underwater image attribute measurement is reverted to in UIQM if two parameters are zero. Multiple Linear Regression (MLR) is used to produce the combination coefficients for broad use.

This work presents a training data set consisting of 30 randomly chosen underwater photos recorded using a variety of equipment at a variety of depths. This manuscript uses the generic coefficients c_1=0.0282, c_2=0.2953, and c_3=3.5753 to get its results. Image enhancing algorithms' effectiveness can be measured using the metrics. Increases in UIQM of 10% are associated with a noticeable improvement in perceived image quality [38].

PCQI: This metric works by dividing the reference and distorted images into patches, and calculating the contrast difference between corresponding patches in the two images. This can be formulated as:

$$\text{PCQI} = \frac{1}{N}\sum[C(i).D(i).F(i)] \tag{14}$$

Consider N as entire count of patches, $C(i)$ as contrast of the reference patch i, $D(i)$as contrast of the distorted patch i; $F(i)$ is a quality pooling function that maps the local contrast differences to a single quality score.

PSNR: The PSNR value is a numerical representation of the ratio betwixt maximum possible value (intensity) of an image and the intensity of deteriorating noise that affects the quality of its categorization. PSNR is typically represented in logarithmic decibel scale since most of the signals having an extraordinarily broad strong range (ratio among the largest and lowermost conceivable estimations of a movable quantity). There must be no visual difference between the elements of the authentic image framework and those of the tainted picture grid [39]. The following equation provides a mathematical expression for the PSNR:

$$\text{PSNR} = 20\ \log_{10}\left(\frac{Max_f}{\sqrt{\text{MSE}}}\right) \tag{15}$$

Max_f implies maximal value of signal in original image and MSE can be given as [40]:

$$\text{MSE} = \frac{1}{mn}\sum_{p=1}^{M}\sum_{q=1}^{N}\big(I(p,q) - J(p,q)\big)^2 \tag{16}$$

Where I and J represents data of original image and restored image respectively.

SSIM: The SSIM metric measures the similarity between two images by comparing their structural information, luminance, and contrast. The resulting SSIM score ranges between -1 and 1, where a score of 1 indicates a perfect match between the two images. The SSIM formula is defined as:

$$\text{SSIM}(x,y) = [I(x,y) * C(x,y) * S(x,y)] \tag{17}$$

Where $I(x,y)$, $C(x,y)$ and $S(x,y)$ are three components that measure the luminance, contrast, and structural similarity between the two images.

AG: It is a measure of the change in intensity values between neighboring pixels in an image. It is often used in image processing tasks, like image enhancement, edge detection. The formula for calculating the average gradient of an image is:

$$\text{AG}(x,y) = \frac{y_i - y_j}{x_i - x_j} \tag{18}$$

Where, (x_i, y_i) corresponds to ith pixel and (x_i, y_i) corresponds to jth pixel of an image.

RMSE: This is used to measure the difference amongst predicted and observed values in a dataset. In the context of image quality enhancement, RMSE is often used to scale the variation amidst the original and enhanced image. It provides a quantitative measure of how much the enhanced image deviates from the original image. The formula for RMSE is:

$$\text{RMSE} = \text{sqrt}\left(\frac{1}{N} * \text{sum}(x_i - y_i^2)\right) \tag{19}$$

Where N denotes number of pixels in the image, x_i denotes pixel value of original image, and y_i denotes corresponding pixel value of the enhanced image.

Sobel Count: The Sobel operator is a common image processing technique used for edge detection as well as image quality enhancement. It is a type of spatial filter that computes the gradient of the image intensity at each pixel location, which can be used to highlight edges and features in the image.

Entropy: This can be used as a metric for measuring the amount of information content in an image. The formula for entropy of an image is given by:

$$H = -\sum(p(x)\log_2 p(x)) \tag{20}$$

Here H indicates entropy, $p(x)$ indicates probability of occurrence of pixel intensity x.

Color enhancement factor (CEF): It helps in the representation of the effect of enhancement and is given as equation (21).

$$\text{CEF} = \frac{\text{CM}(\tilde{I})}{\text{CM}(I)} \tag{21}$$

Where $\text{CM}(I)$ represent the standard deviations, and $\text{CM}(\tilde{I})$ is used to denote enhanced image in the original image.

Contrast to noise ratio (CNR): This metric describes the amplitude of the signal relative to the surrounding noise in an image, and is computed by:

$$\text{CNR}\ (I, I') = \frac{(\mu_i - \mu_n)}{\sigma_n} \tag{22}$$

μ_i represents the mean value of original image and μ_n is mean value of enhanced image and σ_n denotes the standard deviation.

Image enhancement metric (IEM): This metric gives information about the sharpness and the improvement in the contrast after the process of enhancement and computed as follows:

$$\mathrm{IEM} = \frac{\sum_{l=1}^{k_1}\sum_{m=1}^{k_2}\sum_{n=1}^{8}\left|I_{e,c}^{m,l} - I_{e,n}^{m,l}\right|}{\sum_{l=1}^{k_1}\sum_{m=1}^{k_2}\sum_{n=1}^{8}\left|I_{o,c}^{m,l} - I_{o,n}^{m,l}\right|} \tag{23}$$

k_1 and k_2 denote the non-overlapping blocks. o and e represent the original and enhanced images respectively. The intensities of the center pixel is denoted by $I_{o,c}^{m,l}$ and $I_{e,c}^{m,l}$. $I_{o,n}^{m,l}$ and $I_{e,n}^{m,l}$ are the intensities of the neighbors from the center pixel.

Absolute mean brightness error (AMBE): It helps to compute the brightness content that is preserved after the process of image enhancement, denoted as:

$$\mathrm{AMBE}(o,e) = |\mu_o - \mu_e| \tag{24}$$

Equation (23) represents the absolute difference between the mean of original and enhanced images. Median values of AMBE metric indicate good preservation of brightness.

Spatial spectral entropy-based quality index (SSEQ): This is a highly efficient no reference (NR) IQA model. This can assess the quality of an image which is distorted across various distortion categories. SSEQ can be calculated by:

$$\mathrm{SSEQ} = -\sum_{i}\sum_{j} P(i,j)\log_2 P(i,j) \tag{25}$$

Where, $P(i,j)$ is the spectral probability map.

Measure of Enhancement (EME): This calculates the contrast of the images and aids in the optimum selection of processing parameters, and can be computed as:

$$\mathrm{EME} = \max\left(\frac{1}{m_1 m_2}\sum_{l=1}^{m_1}\sum_{n=1}^{m_2} 20\log\frac{X_{\max(n,l)}^{\omega}}{X_{\min(n,l)}^{\omega}}\right) \tag{26}$$

Where, $X_{\max(n,l)}^{\omega}$ and $X_{\min(n,l)}^{\omega}$ represent the maximum value and minimum value of the image within the block $\omega_{n,l}$. m_1 and m_2 represent the blocks in which the image is divided.

Measure of Enhancement by Entropy (EMEE): Good image quality is indicated by high value of EMEE and denoted as:

$$\mathrm{EMEE} = \max\left(\frac{1}{m_1 m_2}\sum_{l=1}^{m_1}\sum_{n=1}^{m_2} \alpha\frac{X_{\max(n,l)}^{\omega}(\theta)}{X_{\min(n,l)}^{\omega}(\theta)}\right) \tag{27}$$

Colourfulness contrast fog density index (CCF): No-reference IQA method is proposed to predict underwater colour image quality using CCF metric. CCF metric is a weighted combination of colourfulness index, contrast index and fog density index which is computed as:

$$\mathrm{CCF} = \omega_1 * \text{colourfulness} + \omega_2 * \text{contrast} + \omega_3 * \text{fog dendisty} \tag{28}$$

Colourfulness index due to absorption, blurring because of forward scattering and fog density due to backward scattering are examined in the CCF computation.

B. Qualitative Analysis

Our testing was conducted in MATLAB® 2021 on a Windows 10 machine equipped with 8 GB RAM and an Intel Core i5 processor. The reference dataset is mined for its colour test photos. A number of cutting-edge methods for improving underwater images, including as DCP, Retinex, and CLAHE, are compared to the suggested method on a qualitative and quantitative scale to gauge its efficacy. In this study, we conduct tests on UIEB dataset [21], which is comprised of 950 photos captured in actual underwater environments. Mean squared Error (MSE), Peak signal-to-noise ratio (PSNR), Underwater Image Quality Measure (UIQM), and Underwater Colour Image Quality Evaluation (UCIQE) are examples of non-reference criteria used for qualitative assessment.

Figure 3 displays the outcomes of various techniques beside their respective benchmark pictures. The UIEB [21] was mined for these test photographs, which were taken in a variety of underwater environments with varying colour palettes and lighting. Underwater photography typically occurs in low light because of the strong absorption of visible light. CLAHE tends to give artificial appearance because the outputs are too bright for visual perception, but the DCP [9], Retinex [8] based, and suggested approaches can generate visually pleasant results. The lack of illumination is too much for CLAHE to process. However, the suggested solution outperforms the reference image in the dark background area when it comes to enhancing details. Pictures taken underwater typically have a greenish or blue tint because light is attenuated at different rates at different wavelengths as illustrated in Fig.3(a). The Retinex's assumptions are very restrictive, exacerbating the impact of colour distortion. The approach is able to efficiently enhance the underwater images contrast, but it is unable to restore the hue of a bluish image, shown as Fig.3(b). The contrast improvement is less successful when using DCP [9] techniques, depicted in Fig.3(c) and the results continue to show haze. In Fig.3(d), though CLAHE [5] seems to be an improvement over the two, Retinex [8] and DCP [9], but it suffers with an over contrast in the picture making it unreliable for specific object detention. The proposed fusion technique of CLAHE [5] and TGV [7] methods achieve similar outcomes to the Retinex-based method but excels in detail preservation. Furthermore, the effectiveness of object detection due to balanced contrast, reducing haze and improving visibility are the achievements of the proposed method as displayed in Fig.3(e). Last but not least, the proposed method works satisfactorily in a wide range of lighting conditions.

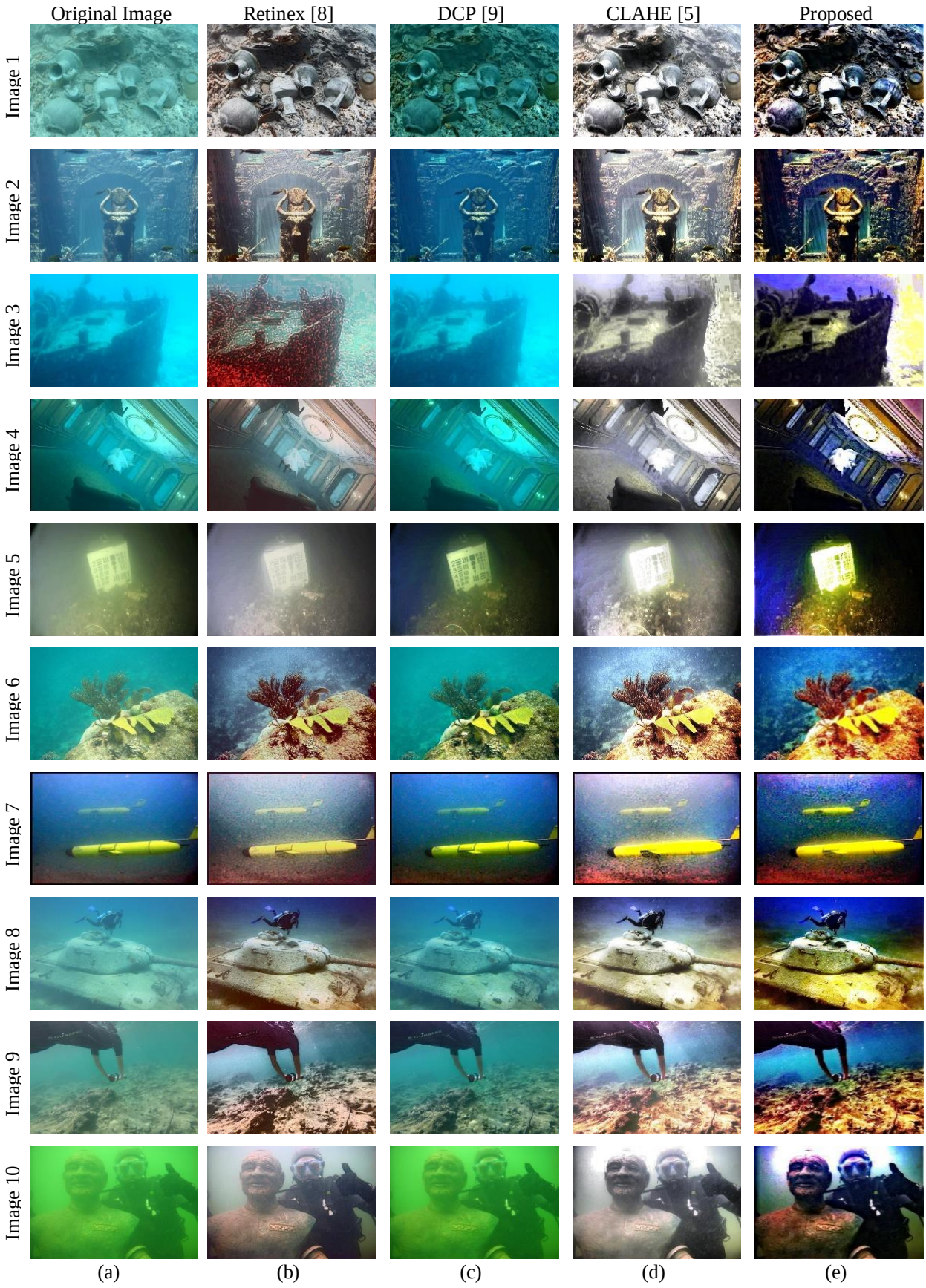

Fig. 3. (a) Original Underwater Images (1st Column) (b-d) Enhanced Images using the existing Retinex [8], DCP [9] and CLAHE [5] methods (2nd, 3rd, 4th Columns) (e) Enhanced Images of the proposed CLAHE+TGV method (5th Column)

TABLE I
QUALITATIVE COMPARISON OF UNDERWATER IMAGES FOR VARIOUS ENHANCEMENT METHODS

Image	Quality Metrics	Retinex [8]	DCP [9]	CLAHE [5]	Proposed
Image 1	UCIQE	0.2557	0.3696	0.2896	0.4384
	UIQM	1.7515	2.3696	1.3071	2.9869
	PCQI	0.2806	0.2992	0.3421	0.45
	PSNR	13.9568	15.6945	23.6859	27.7723
	SSIM	0.2557	0.3057	0.3696	0.4084
	RMSE	200.515	259.28	169.493	96.8415
	AG	95.8415	169.493	200.515	259.28
	Sobel Count	0.2806	0.2992	0.3696	0.4584
	Entropy	0.2806	0.2992	0.3421	0.45
Image 2	UCIQE	0.2685	0.3572	0.3072	0.4399
	UIQM	1.7101	2.3572	1.5093	2.9912
	PCQI	0.2786	0.2999	0.3772	0.449
	PSNR	14.6412	16.5826	17.3945	21.5655
	SSIM	0.2685	0.3185	0.3572	0.4149
	RMSE	210.859	250.9	170.657	95.13
	AG	99.13	170.657	210.859	250.9
	Sobel Count	0.2786	0.2999	0.3572	0.4449
	Entropy	0.2786	0.2999	0.3772	0.449
Image 3	UCIQE	0.2686	0.3545	0.2945	0.4298
	UIQM	1.0576	2.3545	1.6090	2.9931
	PCQI	0.2186	0.2945	0.3216	0.445
	PSNR	15.6516	20.3248	18.3248	26.6631
	SSIM	0.2686	0.3286	0.3545	0.4047
	RMSE	219.657	252.311	178.156	95.183
	AG	95.183	178.156	219.657	252.311
	Sobel Count	0.2186	0.2945	0.3545	0.4449
	Entropy	0.2186	0.2945	0.3216	0.445
Image 4	UCIQE	0.2542	0.3475	0.2975	0.4393
	UIQM	1.4397	2.3475	1.2347	2.9868
	PCQI	0.2844	0.2975	0.3342	0.4593
	PSNR	13.9007	16.2038	20.6313	26.2913
	SSIM	0.2542	0.3142	0.3475	0.4093
	RMSE	205.03	242.49	153.192	97.646
	AG	98.646	153.192	205.03	242.49
	Sobel Count	0.2840	0.2975	0.3475	0.4547
	Entropy	0.2844	0.2975	0.3342	0.4593
Image 5	UCIQE	0.2619	0.3576	0.3076	0.4347
	UIQM	1.7539	2.3576	1.6063	2.9924
	PCQI	0.2652	0.3119	0.3576	0.4447
	PSNR	18.1478	13.7295	17.4739	26.2213
	SSIM	0.2619	0.3219	0.3576	0.4147
	RMSE	220.3695	253.34	120.9442	99.979
	AG	96.979	120.9442	220.3695	253.34
	Sobel Count	0.2652	0.3119	0.3576	0.4493
	Entropy	0.2652	0.3119	0.3576	0.4447
Image 6	UCIQE	0.2526	0.3702	0.3402	0.4376
	UIQM	1.0384	2.3502	1.1897	2.9847
	PCQI	0.3162	0.3426	0.3702	0.4576
	PSNR	13.7701	5.5760	18.8436	25.8372
	RMSE	217.9442	240.431	142.147	98.7601
	AG	94.7601	142.147	217.9442	240.431
	Sobel Count	0.3162	0.3426	0.3502	0.4547
	Entropy	0.3162	0.3426	0.3702	0.4576
Image 7	UCIQE	0.2626	0.3506	0.3806	0.4320
	UIQM	1.6505	2.3606	1.5614	2.9876
	PCQI	0.3042	0.3608	0.3906	0.4499
	PSNR	15.4733	18.0709	19.7016	25.9991
	SSIM	0.2508	0.3308	0.3606	0.4119
	RMSE	217.0377	255.649	125.927	95.8846
	AG	96.884	125.927	217.0377	255.649
	Sobel Count	0.3042	0.3608	0.3606	0.4476
	Entropy	0.3042	0.3608	0.3906	0.4499

Image 8	UCIQE	0.2532	0.3559	0.3359	0.4280
	UIQM	1.5702	2.3559	1.0162	2.9972
	PCQI	0.2226	0.3105	0.3459	0.448
	PSNR	13.3366	18.0469	21.9666	26.2255
	SSIM	0.2626	0.3226	0.3559	0.408
	RMSE	215.575	246.51	138.804	96.2084
	AG	98.2084	138.804	215.57	246.51
	Sobel Count	0.2226	0.3105	0.3559	0.4480
	Entropy	0.2226	0.3105	0.3459	0.4480
Image 9	UCIQE	0.2526	0.3438	0.3138	0.4381
	UIQM	1.2263	2.3438	1.4058	2.9817
	PCQI	0.2432	0.2866	0.3238	0.4491
	PSNR	15.0683	19.8713	16.8908	26.3267
	SSIM	0.2532	0.3232	0.3438	0.4081
	RMSE	208.657	250.72	123.008	96.2084
	AG	99.0941	123.008	208.657	250.72
	Sobel Count	0.2432	0.2866	0.3438	0.4481
	Entropy	0.2432	0.2866	0.3238	0.4491
Image 10	UCIQE	0.2643	0.3571	0.2871	0.4295
	UIQM	1.3005	2.3571	1.0075	2.9841
	PCQI	0.2343	0.2729	0.3271	0.4559
	PSNR	11.9540	26.6846	14.4971	27.2953
	SSIM	0.2643	0.3343	0.3571	0.4105
	RMSE	202.284	250.349	180.89	97.096
	AG	98.096	180.89	202.284	250.349
	Sobel Count	0.2343	0.2729	0.3571	0.4505
	Entropy	0.2343	0.2729	0.3271	0.4559

Table I shows the quantitative comparison of underwater images for the enhancement techniques via Retinex [8], DCP [9], CLAHE [5] and the proposed cascaded combination of CLAHE and TGV methods. The quality metrics UCIQE, UIQM, PSNR and MSE are measured for all the underwater images 1-10 considered. The values are quite interesting in Table I displays that the proposed method outperforms all other methods. A complete analysis of the Quality metrics values obtained are exhibited in bar graphs for comparison among the methods used in this work. Figures 4, 5 and 6 signifies the simulation outcome of full reference analysis (UCIQE, UIQM, PCQI) of proposed CLAHE-TGV compared with existing method such as Retinex [8], DCP [9], and CLAHE [5].

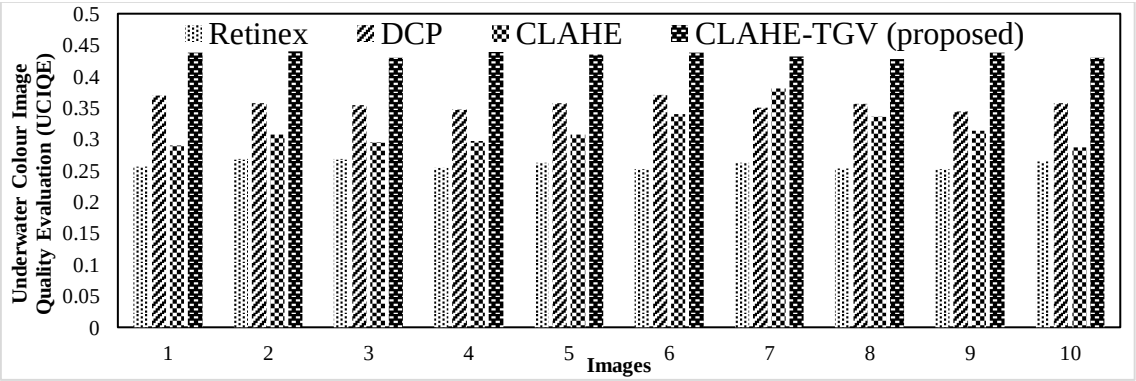

Fig. 4. Analysis of Underwater Colour Image Quality Evaluation (UCIQE) Metric

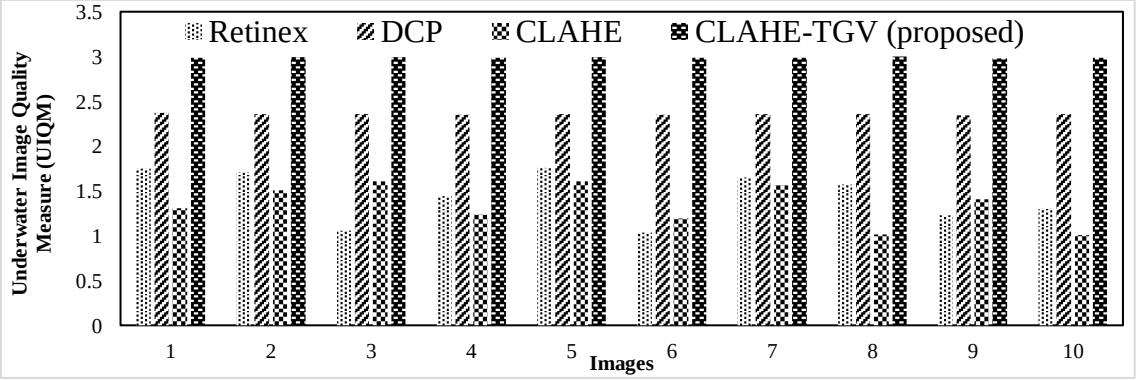

Fig. 5. Analysis of Underwater Image Quality Measure (UIQM)

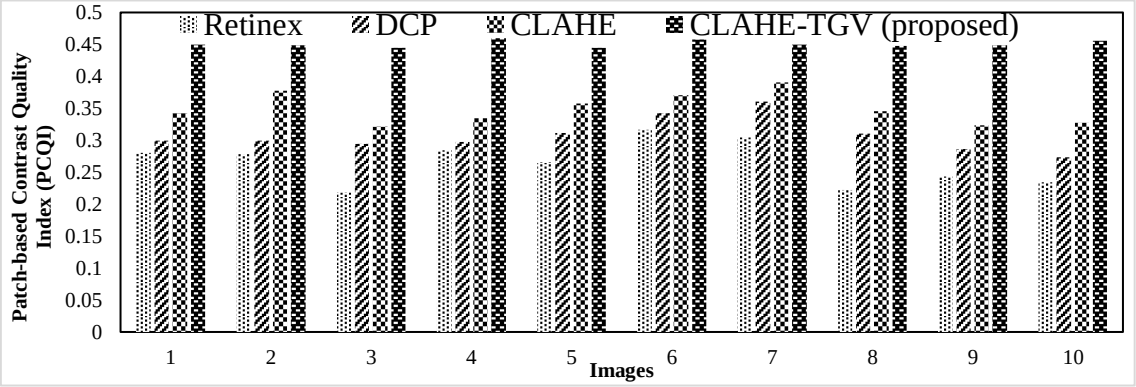

Fig. 6. Analysis of Patch-based Contrast Quality Index (PCQI)

Fig. 4 depicts the analysis of UCIQE. Here the proposed (CLAHE-TGV) method attains 37.65%, 27.76% and 11.56% higher UCIQE for image 2; 22.87%, 38.40% and 47.48% higher UCIQE for image 4; 19.56%, 25.65% and 37.56% higher UCIQE for image 6; 45.45%, 39.65% and 20.43% higher UCIQE for image 8; 28.47%, 38.56% and 58.65% higher UCIQE for image 10, compared with existing method such as Retinex [8], DCP [9], and CLAHE [5] respectively. Figure 5 depicts the analysis of UIQM. Here the proposed (CLAHE-TGV) method attains 37.65%, 27.76% and 11.56% higher UIQM for image 2; 25.67%, 38.40% and 27.38% higher UIQM for image 4; 29.36%, 35.45% and 27.66% higher UIQM for image 6; 25.45%, 19.65% and 30.43% higher UIQM for image 8; 18.47%, 28.56% and 38.65% higher UIQM for image 10, compared with existing method such as Retinex [8], DCP [9], and CLAHE [5] respectively. Figure 6 depicts the analysis of PCQI. Here the proposed (CLAHE-TGV) method attains 12.57%, 24.60% and 31.38% higher PCQI for image 2; 17.65%, 27.36% and 21.46% higher PCQI for image 4; 14.19%, 25.23% and 17.14% higher PCQI for image 6; 28.27%, 18.06% and 18.25% higher PCQI for image 8; 24.65%, 23.36% and 22.11% higher PCQI for image 10, compared with existing method such as Retinex [8], DCP [9], and CLAHE [5] respectively. Figure 6 depicts the analysis of Mean Squared-Error (MSE). Here the proposed (CLAHE-TGV) method attains 32.57%, 44.60% and 51.58% lower MSE for image 2; 27.65%, 17.36% and 31.46% lower MSE for image 4; 24.19%, 35.23% and 27.14% lower MSE for image 6; 18.27%, 38.06% and 28.15% lower MSE for image 8; 14.65%, 27.36% and 32.11% lower MSE for image 10, compared with existing method such as Retinex [8], DCP [9], and CLAHE [5] respectively.

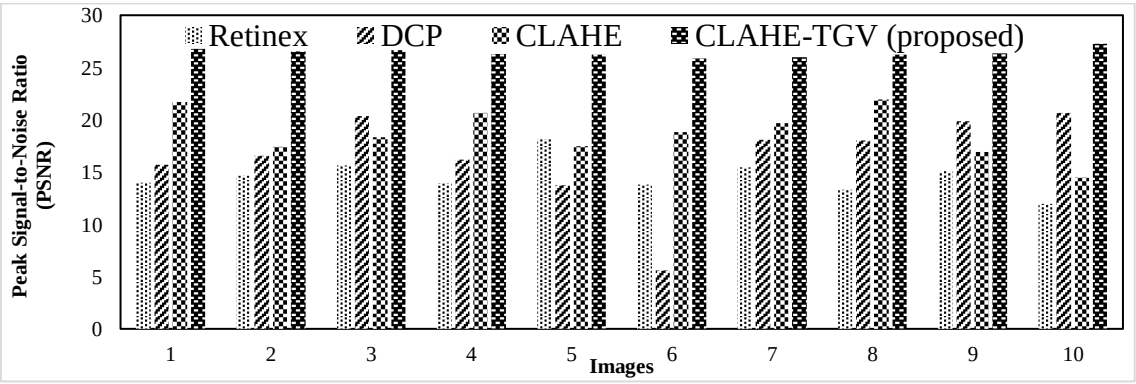

Fig. 7. Analysis of Peak Signal-to-Noise Ratio (PSNR)

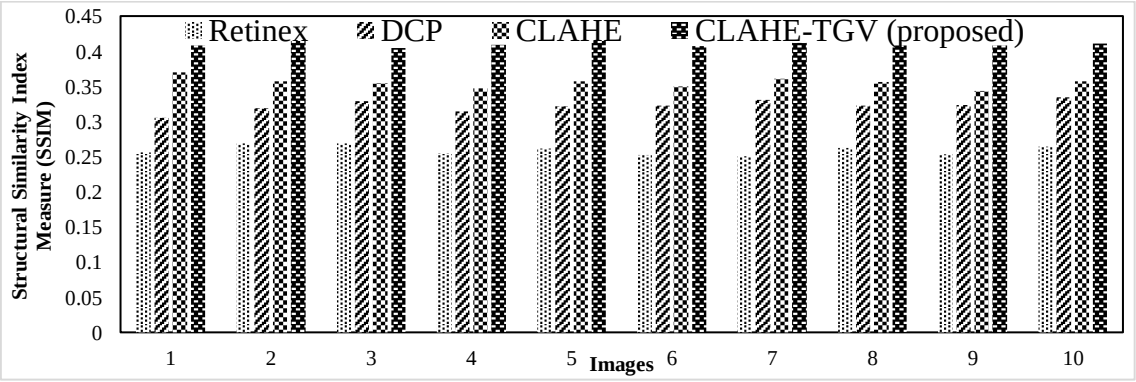

Fig. 8. Analysis of Structural Similarity Index Measure (SSIM)

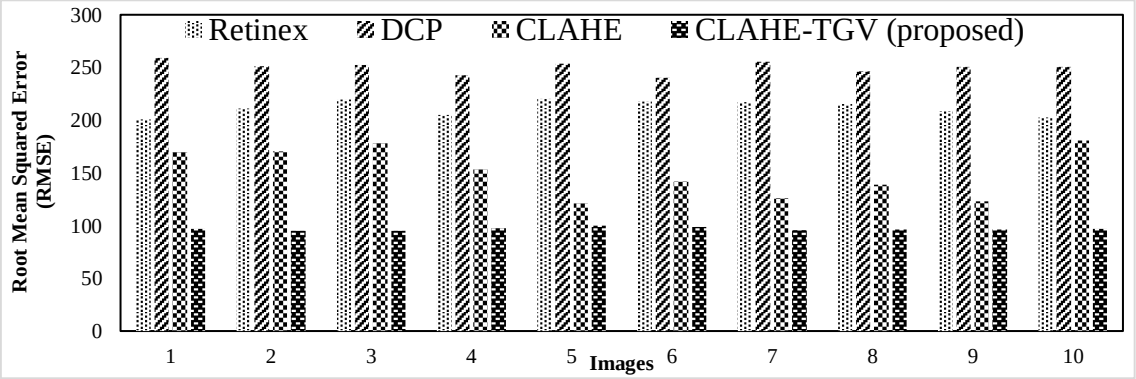

Fig. 9. Analysis of Root Mean Squared Error

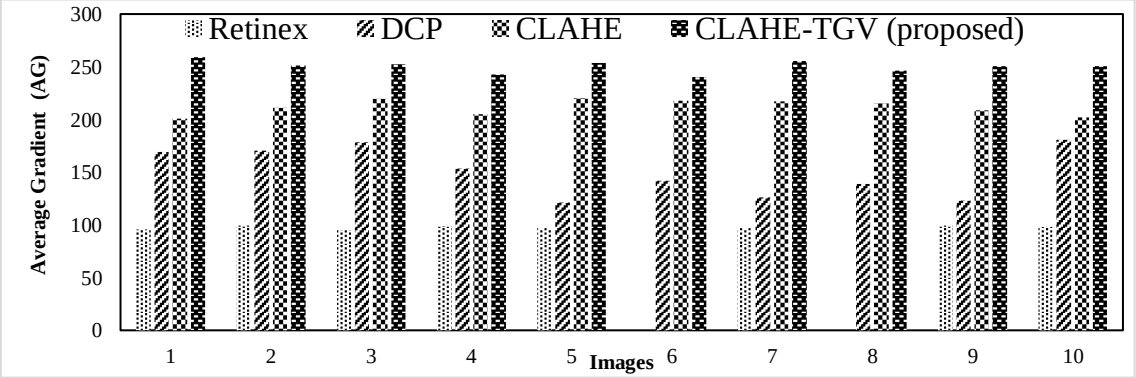

Fig. 10. Analysis of Average Gradient

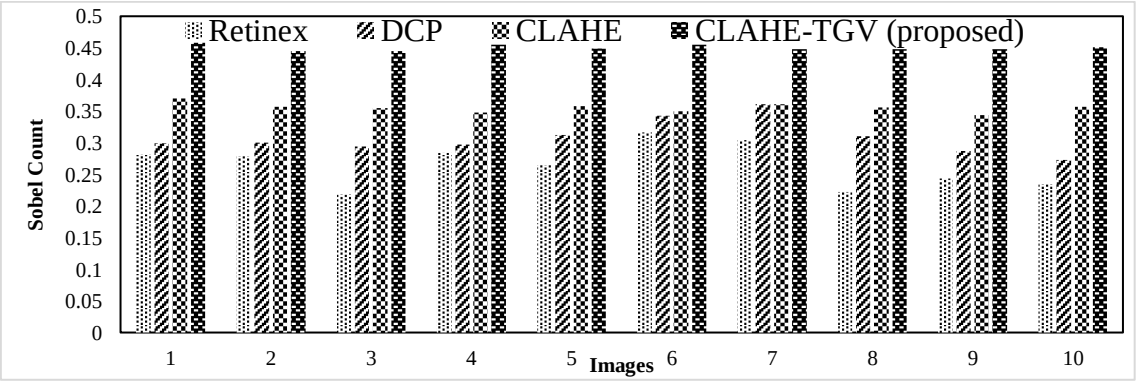

Fig. 11. Analysis of Sobel Count

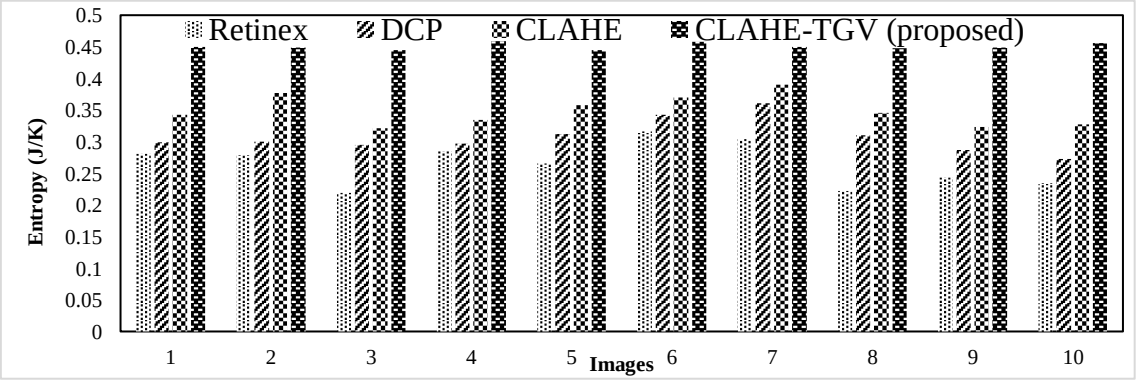

Fig. 12. Analysis of Entropy

Figures 7-12 signifies the simulation outcome of non-reference analysis (PSNR, SSIM, RMSE, AG, Sobel Count, Entropy) of proposed CLAHE-TGV compared with existing method such as Retinex [8], DCP [9], and CLAHE [5]. Figure 7 depicts the analysis of PSNR. Here the proposed (CLAHE-TGV) method attains 27.45%, 28.65% and 25.65% higher PSNR for image 2; 26.45%, 21.56% and 24.56% higher PSNR for image 4; 14.64% 22.45% and 28.56% higher PSNR for image 6; 27.45%, 21.45% and 20.43% higher PSNR for image 8; 17.35%, 18.25% and 15.15% higher PSNR for image 10, compared with existing method such as Retinex [8], DCP [9], and CLAHE [5] respectively. Figure 8 depicts the analysis of Structural Similarity Index Measure (SSIM). Here the proposed (CLAHE-TGV) method attains 24.35%, 22.35% and 21.35% higher SSIM for image 2; 23.45%, 24.45% and 25.33% higher SSIM for image 4; 19.64% 21.45% and 12.56% higher SSIM for image 6; 24.64%, 19.44% and 17.66% higher SSIM for image 8; 24.45%, 22.45% and 28.43% higher SSIM for image 10, compared with existing method such as Retinex [8], DCP [9], and CLAHE [5] respectively. Figure 9 depicts the analysis of RMSE. Here the proposed (CLAHE-TGV) method attains 27.35%, 23.25% and 20.15% lower RMSE for image 2; 21.45%, 20.45% and 16.33% lower RMSE for image 4; 24.64% 14.45% and 18.56% lower RMSE for image 6; 26.45% 18.54% and 19.66% lower RMSE for image 8; 24.45%, 22.45% and 20.43% lower RMSE for image 10, compared with existing method such as Retinex [8], DCP [9], and CLAHE [5] respectively. Figure 10 depicts the analysis of Average Gradient (AG). Here the proposed (CLAHE-TGV) method attains 32.87%, 28.40% and 37.48% higher AG for image 2; 27.35%, 17.26% and 41.16% higher AG for image 4; 54.61%, 65.53% and 37.94% higher AG for image 6; 38.37%, 58.36% and 68.65% higher AG for image 8; 34.65%, 57.26% and 11.66% higher AG for image 10, compared with existing method such as Retinex [8], DCP [9], and CLAHE [5] respectively. Figure 11 depicts the analysis of Sobel count. Here the proposed (CLAHE-TGV) method attains 17.35%, 13.25% and 10.15% higher Sobel count for image 2; 14.45%, 16.45% and 21.33% higher Sobel count for image 4; 14.45%, 16.45% and 21.33% higher Sobel count for image 6; 14.64%, 28.44% and 29.66% higher Sobel count for image 8; 14.45%,12.45% and 18.43% higher Sobel count for image 10, compared with existing method such as Retinex [8], DCP [9], and CLAHE [5] respectively. Figure 12 depicts the analysis of Entropy. Here the proposed (CLAHE-TGV) method attains 42.57%, 48.60% and 57.58% higher Entropy for image 2; 37.65%, 47.16% and 41.16% higher Entropy for image 4; 34.11%, 55.13% and 47.14% higher Entropy for image 6; 28.27%, 48.66% and 58.45% higher Entropy for image 8; 24.65%, 47.56% and 31.56% higher Entropy for image 10, compared with existing method such as Retinex [8], DCP [9], and CLAHE [5] respectively.

Table II depicts the analysis of CEF. Here the proposed (CLAHE-TGV) method attained 17.88%, 25.17% and 18.02% higher CEF for image 2; 18.15%, 12.87% and 10.11% higher CEF for image 4; 28.04%, 23.89% and 29.92% higher CEF for image 6; 20.23%, 14.38% and 11.85% higher CEF for image 8; 22.62%, 28.85% and 7.48% higher CEF for image 10, compared with existing method such as Retinex [8], DCP [9] and CLAHE [5] respectively.

TABLE II
PERFORMANCE ANALYSIS OF CEF

Image	Retinex [8]	DCP [9]	CLAHE [5]	Proposed
1	0.645	0.784	0.871	0.872
2	0.659	0.785	0.759	0.881
3	0.457	0.657	0.713	0.824
4	0.654	0.598	0.214	0.847
5	0.458	0.645	0.567	0.781
6	0.557	0.664	0.567	0.689
7	0.745	0.558	0.287	0.725
8	0.689	0.457	0.554	0.841
9	0.458	0.568	0.687	0.712
10	0.696	0.587	0.597	0.771

TABLE III
PERFORMANCE ANALYSIS OF CNR

Image	Retinex [8]	DCP [9]	CLAHE [5]	Proposed
1	0.754	0.654	0.781	0.872
2	0.549	0.785	0.769	0.871
3	0.257	0.657	0.753	0.854
4	0.564	0.758	0.264	0.867
5	0.578	0.685	0.577	0.791
6	0.667	0.774	0.547	0.789
7	0.855	0.668	0.297	0.765
8	0.779	0.587	0.544	0.881
9	0.598	0.698	0.667	0.792
10	0.796	0.687	0.597	0.781

Table III depicts the analysis of CNR. Here the proposed (CLAHE-TGV) method attained 20.14%, 20.16% and 27.06% higher CNR for image 2; 21.19%, 28.10% and 23.89% higher CNR for image 4; 23.13%, 21.69% and 23.63%% higher CNR for image 6; 21.27%, 15.53% and 27.87% higher CNR for image 8; 25.15%, 22.27% and 24.35% higher CNR for image 10, compared with existing method such as Retinex [8], DCP [9] and CLAHE [5] respectively.

TABLE IV
PERFORMANCE ANALYSIS OF IEM

Image	Retinex [8]	DCP [9]	CLAHE [5]	Proposed
1	0.745	0.814	0.771	0.874
2	0.759	0.825	0.849	0.885
3	0.557	0.757	0.813	0.826
4	0.754	0.698	0.614	0.848
5	0.558	0.745	0.667	0.786
6	0.657	0.764	0.767	0.685
7	0.845	0.658	0.687	0.724
8	0.789	0.557	0.754	0.845
9	0.558	0.668	0.787	0.815
10	0.756	0.687	0.697	0.776

TABLE V
PERFORMANCE ANALYSIS OF AMBE

Image	Retinex [8]	DCP [9]	CLAHE [5]	Proposed
1	0.845	0.684	0.671	0.474
2	0.859	0.585	0.759	0.385
3	0.657	0.557	0.613	0.226
4	0.854	0.798	0.414	0.348
5	0.658	0.545	0.467	0.486
6	0.757	0.664	0.567	0.485
7	0.745	0.658	0.487	0.324
8	0.889	0.457	0.554	0.345
9	0.658	0.768	0.587	0.415
10	0.796	0.587	0.597	0.376

Table IV depicts the analysis of IEM. Here the proposed (CLAHE-TGV) method attained 20.82%, 38.19% and

20.97% higher IEM for image 2; 26.49%, 18.54% and 16.21% higher IEM for image 4; 54.39%, 80.48% and 61.75% higher IEM for image 6; 12.292%, 15.365% and 11.551% higher IEM for image 8; 26.15%, 12.27% and 24.35% higher IEM for image 10, compared with existing method such as Retinex [8], DCP [9] and CLAHE [5] respectively.

Table V depicts the analysis of AMBE. Here the proposed (CLAHE-TGV) method attained 27.86%, 35.85% and 27.86% lower AMBE for image 2; 32.85%, 29.07% and 32.86% lower AMBE for image 4; 32.86%, 28.97% and 44.85% lower AMBE for image 6; 28.97%, 34.97% and 27.97% lower AMBE for image 8; 33.86%, 28.97%, and 36.97% lower AMBE for image 10, compared with existing method such as Retinex [8], DCP [9] and CLAHE [5] respectively.

TABLE VI
PERFORMANCE ANALYSIS OF SSEQ

Image	Retinex [8]	DCP [9]	CLAHE [5]	Proposed
1	0.58	0.61	0.74	0.84
2	0.69	0.52	0.47	0.89
3	0.47	0.43	0.41	0.86
4	0.78	0.78	0.85	081
5	0.58	0.45	0.52	0.89
6	0.69	0.59	0.86	0.84
7	0.45	0.48	0.65	0.85
8	0.69	0.67	0.56	0.86
9	0.57	0.55	0.24	0.91
10	0.59	0.78	0.46	0.88

Table VI depicts the analysis of SSEQ. Here the proposed (CLAHE-TGV) method attained 33.86%, 28.97%, and 36.97% higher SSEQ for image 2; 43.86%, 37.97%, and 37.97% higher SSEQ for image 4; 44.97%, 36.97%, and 28.97% higher SSEQ for image 6; 43.87%, 26.87%, and 29.98% higher SSEQ for image 8; 33.75%, 27.98%, and 36.97% higher SSEQ for image 10, compared with existing method such as Retinex [8], DCP [9] and CLAHE [5] respectively.

TABLE VII
PERFORMANCE ANALYSIS OF EME

Image	Retinex [8]	DCP [9]	CLAHE [5]	Proposed
1	0.68	0.71	0.64	0.85
2	0.79	0.62	0.57	0.87
3	0.57	0.53	0.51	0.88
4	0.88	0.88	0.75	0.92
5	0.68	0.55	0.62	0.87
6	0.79	0.69	0.76	0.85
7	0.55	0.58	0.75	0.86
8	0.79	0.77	0.66	0.87
9	0.67	0.65	0.34	0.92
10	0.69	0.68	0.56	0.87

Table VII depicts the analysis of EME. Here the proposed (CLAHE-TGV) method attained 25.87%, 26.54%, and 32.87% higher EME for image 2; 32.06%, 20.94% and 32.04% higher EME for image 4; 41.26%, 73.10%, and 24.12% higher EME for image 6; 31.14%, 14.88% and 33.27% higher EME for image 8; 13.75%, 37.98%, and 46.97% higher EME for image 10, compared with existing method such as Retinex [8], DCP [9] and CLAHE [5] respectively.

TABLE VIII
PERFORMANCE ANALYSIS OF EMEE

Image	Retinex [8]	DCP [9]	CLAHE [5]	Proposed
1	0.48	0.71	0.74	0.82
2	0.59	0.42	0.47	0.84
3	0.37	0.23	0.81	0.86
4	0.48	0.58	0.55	0.92
5	0.78	0.85	0.22	0.81
6	0.59	0.69	0.66	0.85
7	0.75	0.68	0.35	0.83
8	0.59	0.87	0.46	0.84
9	0.77	0.55	0.54	0.91
10	0.79	0.28	0.66	0.85

Table VIII depicts the analysis of EMEE. Here the proposed (CLAHE-TGV) method attained 11.2%, 16.35% and 17.7% higher EMEE for image 2; 11.17%, 14.12% and 24.15% higher EMEE for image 4; 22.42%, 36.12% and 15.16% higher EMEE for image 6; 36.22%, 34.55% and 30.8% higher EMEE for image 8; 34.14%, 24.10%, and 21.34% higher EMEE for image 10, compared with existing method such as Retinex [8], DCP [9] and CLAHE [5] respectively.

TABLE IX
PERFORMANCE ANALYSIS OF CCF

Image	Retinex [8]	DCP [9]	CLAHE [5]	Proposed
1	0.58	0.81	0.64	0.92
2	0.69	0.52	0.57	0.87
3	0.47	0.33	0.71	0.84
4	0.58	0.68	0.45	0.92
5	0.88	0.75	0.32	0.88
6	0.69	0.79	0.76	0.89
7	0.85	0.78	0.45	0.86
8	0.69	0.77	0.56	0.83
9	0.87	0.65	0.64	0.95
10	0.89	0.38	0.76	0.82

Table IX depicts the analysis of CCF. Here the proposed (CLAHE-TGV) method attains 28.46%, 33.16% and 20.63% higher CCF for image 2; 26.22%, 14.55% and 20.8% higher CCF for image 4; 34.19%, 29.10%, and 21.3% higher CCF for image 6; 28.43%,33.12% and 20.13% higher CCF for image 8; 16.18%, 24.41% and 21.18% higher CCF for image 10, compared with existing method such as Retinex [8], DCP [9] and CLAHE [5] respectively.

C. Discussion

The efficacy of proposed technique is comparing to the state-of-the art models, like Retinex [8], DCP [9] and CLAHE [5]. Qualitatively and quantitatively evaluate the image quality of each method. In qualitative estimation, colour cast, contrast, and under- and over-enhancing effects are the major factors in deciding resultant image superiority. In contrast, qualitative perceptions are supported by quantitative measurement. The effectiveness of each method is evaluated quantitatively using a variety of evaluation metrics, including UCIQE, UIQM, PCQI, PSNR, SSIM, RMSE, AG, Sobel count and Entropy. To estimate the details of image, entropy is used. It is preferable to have a high entropy number because it shows the image has lot of information. In the meantime, the average gradient displays an image's level of contrast. An image with higher average gradient value will have better contrast and a higher intensity level. Additionally, Sobel edge detection is used to assess the superiority of final image by locating the object's

boundary. Because the borders of the object are clearly detected by the higher value of Sobel edge detection, the resultant image is superior. PCQI is a general-purpose image contrast metric that assess the contrast quality. UIQM is structured to estimate underwater imagery, wherein it considers colourful, sharpness and contrast. Larger PCQI along UIQM values display feasible image superiority. NIQE is the final metric for evaluation, and it contrasts the output image with a default mode created using images from natural scenes. Smaller NIQE displays good image superiority. Here, diverse underwater imageries are employed for testing as well as comparison. These underwater imageries affecting through underwater colour cast, consequently poor contrast occurs. The majority of objects are toughly distinguishable from the background and have very poor visibility levels as a result. Here, 10 images are selected for discussion. The resultant imageries created by every model are depicted in Figures 4 to 13. The histograms of every colour channel including respective histograms mean values are involved for general discussion.

VI. Conclusion

Underwater scenes present a significant challenge for image processing due to the difficulty in distinguishing foreground and background images at varying distances. There are numerous techniques for enhancing underwater images, but they all have considerable limitations. The proposed method incorporates the benefits of both Total Generalized Variation and Contrast Enhancement techniques. We have analyzed the outcome of the proposed technique and compared its performance to the previously existing methods. The quality measures UCIQE and UIQM achieved a greater average value of 0.3658 and 2.0710 respectively, for all the images considered. The PSNR of 22.4350 and MSE value of 80.2131 (both values averaged for all the images 1-10) also show a great reduction in the noise component of the enhanced images through this technique. Hence, the proposed method for removing image haze is both simpler and more efficient than previous methods. There is still a need for a comprehensive database of test photos for various imaging circumstances to improve underwater image processing. Though this technique is applicable to any underwater image, but additional study is required to develop a way to restore colour in underwater images captured at greater depths.

References

[1] Raveendran, S., Patil, M.D. and Birajdar, G.K., 2021. Underwater image enhancement: a comprehensive review, recent trends, challenges and applications. Artificial Intelligence Review, 54, pp.5413-5467.

[2] S. Raveendran, M. Patil and G. K. Birajdar, "Underwater image enhancement: a comprehensive review, recent trends, challenges and applications," *Artificial Intelligence Review*, vol. 54, no. 1, pp. 5413-5467, 2021, doi: 10.1007/s10462-021-10025-z.

[3] Moghimi, M.K. and Mohanna, F., 2021. Real-time underwater image enhancement: a systematic review. *Journal of Real-Time Image Processing*, pp.1-17.

[4] Li, C., Anwar, S., Hou, J., Cong, R., Guo, C. and Ren, W., 2021. Underwater image enhancement via medium transmission-guided multi-color space embedding. *IEEE Transactions on Image Processing*, *30*, pp.4985-5000.

[5] Zhuang, P., Li, C. and Wu, J., 2021. Bayesian retinex underwater image enhancement. *Engineering Applications of Artificial Intelligence*, *101*, p.104171.

[6] X. Ding, Z. Liang, Y. Wang and X. Fu, "Depth-aware total variation regularization for underwater image dehazing," *Signal Processing: Image Communication*, 98, 2021, doi: 10.1016/j.image.2021.116408.

[7] Zhou, J., Zhang, D. and Zhang, W., 2022. Underwater image enhancement method via multi-feature prior fusion. *Applied Intelligence*, pp.1-23.

[8] Jiang, Q., Zhang, Y., Bao, F., Zhao, X., Zhang, C. and Liu, P., 2022. Two-step domain adaptation for underwater image enhancement. *Pattern Recognition*, *122*, p.108324.

[9] Jiang, Q., Gu, Y., Li, C., Cong, R. and Shao, F., 2022. Underwater image enhancement quality evaluation: Benchmark dataset and objective metric. *IEEE Transactions on Circuits and Systems for Video Technology*, *32*(9), pp.5959-5974.

[10] S. N. Ghate and M. D. Nikose, "New Approach to Underwater Image Dehazing using Dark Channel Prior," *Journal of Physics: Conference Series*, pp. 1-16, 2021, doi: 10.1088/1742-6596/1937/1/012045.

[11] W. Song, Y. Wang, D. Huang, A. Liotta and C. Perra, "Enhancement of Underwater Images with Statistical Model of Background Light and Optimization of Transmission Map," *IEEE Transactions on Broadcasting*, vol. 66, no. 1, pp. 153-169, 2020, doi: 10.1109/TBC.2019.2960942.

[12] Yue Zhang, Fuchun Yang and Weikai He. "An approach for underwater image enhancement based on color correction and dehazing," *International Journal of Advanced Robotic Systems*, Vol. 17, no. 5, pp1–10, 2020, doi:10.1177/1729881420961643.

[13] M. Mangeruga, F. Bruno, M. Cozza, P. Agrafiotis, and D. Skarlatos, "Guidelines for Underwater Image Enhancement Based on Benchmarking of Different Methods," *Remote Sensing*, vol. 10, no. 10, p. 1652, 2018, doi: 10.3390/rs10101652.

[14] Sangeetha Mohan and Philomina Simon, "Underwater Image Enhancement based on Histogram Manipulation and Multiscale Fusion," *Procedia Computer Science*, Vol. 171, pp. 941–950, 2020, doi: 10.1016/j.procs.2020.04.102.

[15] Aashi Singh Bhadouria and Khushboo Agarwal, "Effective Framework for Underwater Image Enhancement using Multi-Fusion Technique," *IEEE 9th International Conference on Communication Systems and Network technologies (CSNT)*, pp. 290-295, 2020, doi: 10.1109/CSNT48778.2020.9115777.

[16] A. D. Belsare, Tushar Gathe, and Ankit Charde, "Underwater Image Enhancement Algorithm for Real Time Monitoring and Surveillance," *2019 IEEE 4th International Conference on Recent Trends on Electronics, Information, Communication & Technology (RTEICT)*, pp. 1404-1408, 2019, doi: 10.1109/RTEICT46194.2019.9016755.

[17] Aruna Bhat, Aadhar Tyagi and Aarsh Verdhan, "Fast Under Water Image Enhancement for Real Time Applications," *6th IEEE International Conference for Convergence in Technology (I2CT)*, pp. 1-8, 2021, doi: 10.1109/I2CT51068.2021.9417963.

[18] Sun Bo, Wu Yanxiao, Xue Yawen and Yang Xiangguo, "Underwater Image Enhancement Algorithm Based on Illuminance Domain Analysis," *2021 IEEE International Conference on Power Electronics, Computer Applications (ICPECA)*, pp. 656-661, 2021, doi: 10.1109/ICPECA51329.2021.9362646.

[19] Sourav De, Sandip Dey and Shouvik Paul, "Underwater Image Enhancement Using Neighbourhood based Two Level Contrast Stretching and Modified Artificial Bee Colony," *IEEE 7th Uttar Pradesh Section International Conference on Electrical, Electronics and Computer Engineering (UPCON)*, pp.1-6, 2020, doi: 10.1109/UPCON50219.2020.9376405.

[20] C. Li, C. Guo, W. Ren, R. Cong, J. Hou, S. Kwong and D. Tao, "An Underwater Image Enhancement Benchmark Dataset and Beyond," *IEEE Transactions on Image Processing*, Vol. 29, pp. 4376-4389, 2020, doi :10.1109/TIP.2019.2955241.

[21] G. Ramkumar, G. Anitha, M. Suresh kumar, M. Ayyadurai and C. Senthil kumar, "An Effectual Underwater Image Enhancement using Deep Learning Algorithm," *5th IEEE International Conference on Intelligent Computing and Control Systems (ICICCS)*, pp. 1507-1511, 2021, doi: 10.1109/ICICCS51141.2021.9432116.

[22] Lixue Xu, Xiubo Wang and Xudong Wang, "Underwater Image Enhancement of Improved Retinex Base on Statistical Learning," *8th IEEE Data Driven Control and Learning Systems Conference (DDCLS)*, pp. 1027-1032, 2019, doi: 10.1109/DDCLS.2019.8908885.

[23] Sonal Yadav and Krishna Raj, "Underwater Image Enhancement via Color Balance and Stationary Wavelet Based Fusion," *IEEE International Conference for Innovation in Technology (INOCON)*, pp. 1-5, 2020, doi: 10.1109/INOCON50539.2020.9298231.

[24] Z. Zhao, Y. Dai and P. Zhuang, "Underwater Image Enhancement with a Total Generalized Variation Illumination Prior," 2019 IEEE International Conference on Parallel & Distributed Processing with Applications, Big Data & Cloud Computing, Sustainable Computing

& Communications, Social Computing & Networking, pp. 1041-1048, 2019, doi: 10.1109/ISPA-BDCloud-SustainCom-SocialCom48970.2019.00149.
[25] D. Akkaynak and T. Treibitz, "A Revised Underwater Image Formation Model," Proceedings of the IEEE Conference on Computer Vision and Pattern Recognition (CVPR), pp. 6723-6732, 2018, doi: 10.1109/CVPR.2018.00703.
[26] Y. Cho and A. Kim, "Visibility enhancement for underwater visual SLAM based on underwater light scattering model," 2017 IEEE International Conference on Robotics and Automation (ICRA), pp. 710-717, 2017, doi: 10.1109/ICRA.2017.7989087.
[27] D. Akkaynak, T. Treibitz, T. Shlesinger, R. Tamir, Y. Loya, and D. Iluz, "What is the space of attenuation coefficients in underwater computer vision?" *Proceedings of the IEEE Conference on Computer Vision and Pattern Recognition (CVPR)*, pp. 4931-4940, 2017, doi: 10.1109/CVPR.2017.68.
[28] J. Y. Chiang and Y. C. Chen, "Underwater image enhancement by wavelength compensation and dehazing," *IEEE Transactions on Image Processing*, vol. 21, no. 4, pp. 1756-1769, 2012, doi: 10.1109/TIP.2011.2179666.
[29] A. L. Alldredge and M. W. Silver, "Characteristics, dynamics and significance of marine snow," *Progress in Oceanography*, Vol. 20, pp. 41-82, 1988, doi: 10.1016/0079-6611(88)90053-5.
[30] B. McGlamery, "A computer model for underwater camera systems," *International Society for Optics and Photonics*, Ocean Optics VI, vol. 208, pp. 221–231, 1980, doi: 10.1117/12.958279.
[31] Z. Mi, Y. Li, Y. Wang and X. Fu, "Multi-Purpose Oriented Real-World Underwater Image Enhancement," *IEEE Access*, vol. 8, pp. 112957-112968, 2020, doi: 10.1109/ACCESS.2020.3002883.
[32] Codruta O. Ancuti, Cosmin Ancuti, Christophe De Vleeschouwer and Philippe Bekaert, "Color Balance and Fusion for Underwater Image Enhancement," *IEEE Transactions on Image Processing*, vol. 27, no. 1, pp. 379-393, 2018, doi: 10.1109/TIP.2017.2759252.
[33] Xinwei Xue, Zexuan Li, Long Ma, Qi Jia, Risheng Liu and Xin Fan, "Investigating Intrinsic Degradation Factors by Multi-Branch Aggregation for Real-world Underwater Image Enhancement," *Pattern Recognition*, Vol. 133, 2022, doi: 10.1016/j.patcog.2022.109041.
[34] Jianguang Zhu, Kai Li and Binbin Hao, "Image Restoration by Second-Order Total Generalized Variation and Wavelet Frame Regularization," *Complexity*, pp. 1-16, 2019, doi: 10.1155/2019/3650128.
[35] Leonid I. Rudin, Stanley Osher and Emad Fatemi, "Nonlinear total variation-based noise removal algorithms," *Physica D: Nonlinear Phenomena*, Vol. 60, no. 1-4, pp. 259-268, 1992, doi: 10.1016/0167-2789(92)90242-F.
[36] Z. Liu, Y. Li, W. Wang, L. Liu and R. Chen, "Mesh Total Generalized Variation for Denoising," IEEE Transactions on Visualization and Computer Graphics, vol. 28, no. 12, pp. 4418-4433, 2022, doi: 10.1109/TVCG.2021.3088118.
[37] K. Panetta, C. Gao and S. Agaian, "Human-Visual-System-Inspired Underwater Image Quality Measures," *IEEE Journal of Oceanic Engineering*, vol. 41, no. 3, pp. 541-551, 2016, doi: 10.1109/JOE.2015.2469915.
[38] E. S. Malinverni, C. Cerrano, U. Pantaleo, C Andreola, M Paolanti, S. Chiappini and R. Pierdicca, "Image enhancement comparison to improve underwater cultural heritage survey," *IOP Conference Series: Materials Science and Engineering*, Vol. 949, pp. 1-8, 2020, doi: 10.1088/1757-899X/949/1/012102.
[39] Vamsidhar A., Surya Kavitha T. and Ramesh Babu G., "Image Enhancement Using Chicken Swarm Optimization," *Proceedings of the International Conference on Computational Intelligence and Sustainable Technologies*, pp. 555-565, 2022, doi: 10.1007/978-981-16-6893-7_49.
[40] T. S. Kavita and K. S. Prasad, "Quantitative Comparison of Reconstruction methods for Compressive Sensing MRI," *International Journal of Scientific & Technology Research*, vol. 8, pp. 1504-1508, 2019.

AUTHOR PROFILES

Mrs. T. Surya Kavita received her B.Tech and M.Tech Degrees in ECE from JNTU, Kakinada, India in 2000 and 2003 respectively, and presently pursuing Ph.D. in ECE department, JNTU, Kakinada, India. She has a total experience of 18 years in Teaching. She published more than 20 papers in various International and National journals. Her Research interests are Image Processing, Signal Processing, Swarm Intelligence and Communications.

Dr. A. Vamsidhar received his B.Tech (ECE) from JNTU, Kakinada in 2000 and M.Tech (ECE) from NIT, Calicut, in 2003. He received his Ph.D. from Andhra University, Visakhapatnam, India in 2018. He has more than 20 years of teaching experience in various academic institutions. He published more than 35 papers in various International and National journals and filed 2 patents. His areas of research include Signal, Image processing, Machine Learning and Wireless Communications.

Mr. G. Sunil Kumar received his B.Tech. (ECE) and M.Tech. (ECE) from GIET, Gunupur, Odisha in 2008 and 2012 respectively, and presently pursuing Ph.D. in University of Technology, Jaipur. He has more than 14 years of teaching experience in various academic institutions. He has authored 6 technical publications. His current research interests include Wireless Sensor Networks, Image processing and Swarm Intelligence.

Dr. R. Viswanadham received his B.Tech. (EIE) from JNTU, Hyderabad, India in 2009 and M.Tech. (Embedded Systems) from JNTU, Kakinada, India, in 2011. He completed his Ph.D. from Centurion University of Technology & Management, Odisha, India in 2022. His areas of research include Signal and Speech Processing, Wireless Communications, Machine Learning and Pattern Recognition.

Mr. V. Anand Kumar completed his four year bachelor degree (B.Tech) in the stream of ECE department from Raghu Engineering College, Visakhapatnam, India from 2018-2022. He worked on many case studies in different Signal Processing domains, and participated in many project presentations. His research interests are Image and Signal processing.

Ms. T. Madhuri received her Diploma Degree in ECE from SBTET, Andhra Pradesh, India from 2016-2019 and completed her B.Tech in the stream of ECE department from Raghu Engineering College, Visakhapatnam, India from 2019-2022. She had done various projects and mostly interested in Image and Signal Processing.